© 2011 The Chemical Society of Japan

BCSJ Award Article

Spectroscopic Visualization of Right- and Left-Handed Helical Alignments of DNA in Chiral Vortex Flows

Yuya Tsujimoto, Machiko Ie, Yasunari Ando, Taiki Yamamoto, and Akihiko Tsuda*

Department of Chemistry, Graduate School of Science, Kobe University, 1-1 Rokkodai-cho, Nada-ku, Kobe 657-8501

Received June 8, 2011; E-mail: tsuda@harbor.kobe-u.ac.jp

In a vortex generated by mechanical rotary stirring in an optical cell, DNA molecules in pure water temporarily align helically to the spiral flow, and dynamically display strong induced circular dichroism (CD) and linear dichroism (LD) responses. Although a sample solution without stirring provided the characteristic CD spectral pattern of DNA, an entirely different macroscopic CD spectral pattern with a much larger intensity and LD spectrum appeared upon mechanical rotary stirring of the sample solution. Clockwise (CW) and counterclockwise (CCW) stirring resulted in mirror-image CD spectral profiles and virtually the same LD profiles with different intensities. The CW stirring of the sample solution in LD spectroscopy always resulted in larger spectral intensities than CCW stirring, but the differences became negligible upon addition of NaCl or ethidium bromide. The observed CD and LD responses of the stirred sample solution decreased simultaneously as the double-stranded structure denatures with increasing temperatures. The results obtained in this study indicate that DNA, when it forms a double-stranded structure, can effectively align in the vortex flows, and show hydrodynamic preference to a right-handed vortex than to a left-handed vortex.

Chiral hydrodynamic interactions between DNA and macroscopic torsional fluids attract considerable interest because of the involvement of microscopic and macroscopic chirality in biomolecular systems. DNA can hydrodynamically align and stretch in certain linear fluid flows,[1–5] where a worm-like chain model can reasonably account for the elastic behaviors and hydrodynamic interactions of DNA.[6] Here, as an innovative subject related to those studies, we noticed for the torsional flow dynamics of DNA, having a right-handed helical double-stranded structure, in chiral fluids such as a vortex that is recognized as one possible origin of chiral symmetry breaking in nature.[7–10] Strick et al. reported the first single-molecule measurements of DNA topology using magnetic tweezers; they measured the extension and force of individual λ-phage DNA molecules and found that positively supercoiled DNA was more difficult to stretch than negatively supercoiled DNA.[11] Other studies have also demonstrated experimentally the intrinsic chiral twist elasticity of DNA.[12–15] These studies raise an important question: What happens to DNA in a chiral macroscopic vortex generated by clockwise (CW) or counterclockwise (CCW) stirring? The present study reports a successful spectroscopic visualization of macroscopic helical alignments of DNA in a vortex. DNA, when it forms a double-stranded structure, can effectively align in the vortex flows, and it shows hydrodynamic preference to a right-handed vortex than to a left-handed vortex.

It is known that certain achiral molecules form optically active assemblies in torsional fluids generated upon rotary stirring.[9,10] Kaizu and co-workers[10a] and Ribó and co-workers[10b–10d] have reported pioneering examples in which electrostatic J-aggregates of (4-sulfophenyl)porphyrin derivatives, prepared in aqueous media upon rotary stirring, are optically active. They claimed that hydrodynamic selection of either the right- or left-handed helical conformation of the aggregates is responsible for the optical activity. In fact, the formation of helical ribbons in a stirred solution has recently been confirmed.[10c] These studies have attracted interest in light of possible hydrodynamic interaction between the macroscopic torsional flows and nanoscale molecular assemblies beyond Brownian motions of the solvent molecules. With this background, recently, we have succeeded in spectroscopically visualizing a macroscopic helical alignment of artificial nanofibers, composed of self-assembled zinc porphyrin derivatives, in a vortex.[16,17] Strong linear dichroism (LD) and macroscopic circular dichroism (CD), which may originate from artifactual combinations of linear dichroism (LD), linear birefringence (LB), and circular birefringence (CB),[18] reversibly appear while the sample solutions were stirred in the CW or CCW directions. Here the CW and CCW were defined as rotating direction of the stir bar relative to the gravity axis, and generate right- and left-handed vortex flow, respectively. The hydrodynamic interaction between supramolecular nanofibers 2–10 nm diameter, and solvent molecules may allow their helical alignments in the vortex flow. This finding then prompted us to extend this phenomenon to natural bionanofibers such as DNA, having a diameter of 2.2–2.6 nm. In the

Published on the web September 15, 2011; doi:10.1246/bcsj.20110178

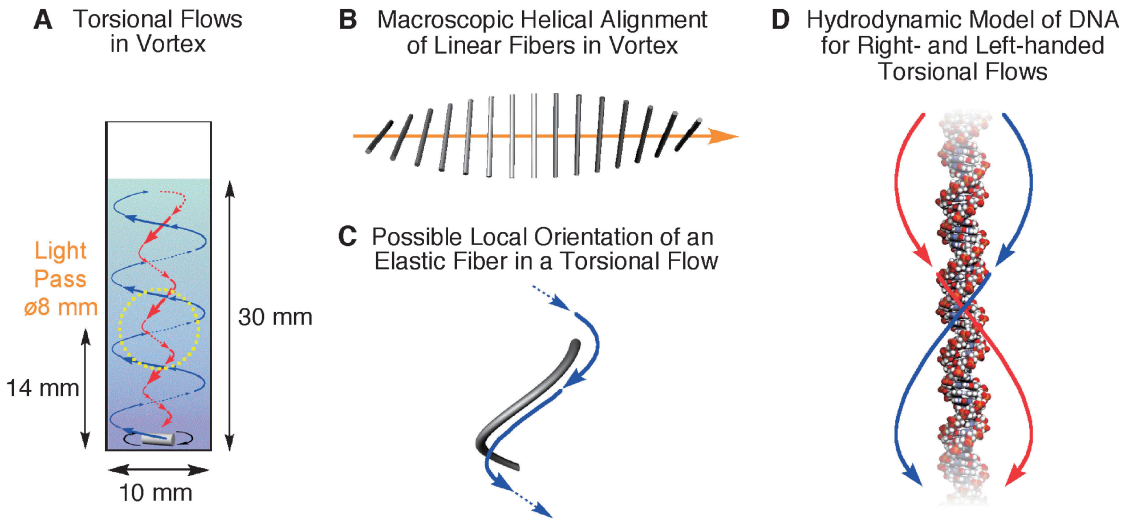

Figure 1. Theoretical predictions of vortex flows generated by mechanical rotary stirring and chiral hydrodynamic models of DNA in the torsional flows. (**A**) Schematic illustration of a sample solution with rotary CW stirring in a $10 \times 10 \times 40\,mm^3$ quartz optical cell containing a magnetic stir bar. For CD and LD spectroscopy, an $\phi 8.0$ mm wide circularly polarized light is allowed to pass through the sample solution at a position 14 mm above the bottom of the inner surface of the optical cell. Schematic illustrations of (**B**) a macroscopic helical alignment of multiple fibers in vortex as light passes during spectroscopy and (**C**) (*P*)-helical deformation of an elastic fiber at the vortex center. (**D**) Hydrodynamic model of DNA with right- and left-handed (blue and red, respectively) torsional flows.

present study, we found that DNA in a water solution without buffer salts results in completely reversible strong, induced CD and LD responses upon CW or CCW rotary stirring. CW stirring of the sample solution always resulted in larger spectral intensities than CCW stirring, but the differences became negligible upon addition of NaCl or ethidium bromide (ETB).

Results and Discussion

CD and LD Spectroscopy of DNA Solutions upon Mechanical Rotary Stirring. The combination of CD and LD spectroscopy can reveal helical deformations and the orientation of anisotropic macromolecules.[16–19] The spectrometer was equipped with a $10 \times 10 \times 40\,mm^3$ quartz optical cell, in which sample solutions (3 mL) were stirred mechanically using a $\phi 3.0 \times 8.0$ mm Teflon-coated magnetic stir bar at the bottom of the cell, 14 mm below the center of a $\phi 8.0$ mm-wide polarized light pass (Figure 1A). An aqueous solution of salmon testes DNA ($5.1 \times 10^{-2}\,mg\,mL^{-1}$), having linear structures with an average molecular weight of approximately $M_w = 1.3 \times 10^6$ (2000 bp),[20] was prepared with ultrapure water without buffer salt and provided the characteristic CD spectral pattern of DNA with peak maxima of $\lambda_{max} = 247$ and 279 nm with intensities of −8.8 and 8.3 mdeg, respectively (Figure 2A, CD, black curve). However, upon mechanical rotary stirring of the sample solution at 1350 rpm, an entirely different CD spectral pattern with a much larger intensity appeared at λ_{max} of 266 nm (Figure 2A, CD, blue and red curves). The sample solution was LD silent without stirring, and it became LD active upon rotary stirring (Figure 2A, LD), the intensity increasing sigmoidally with increasing rotating speed of the stirrer (Figure 3A) and the profile observed is similar to the case of our previously reported supramolecular nanofibers composed of zinc porphyrin dendrimers. The observed LD has positive sign at λ_{max} of 259 nm, indicating vertical alignment of DNA in the vortex, where DNA molecules may hydrodynamically undergo strong torsional downward force in the center of the vortex as schematically illustrated in Figures 1B and 1C.[4,5] The observed spectral intensity was decreased by using a small ($\phi 2.0 \times 5.0$ mm) stir bar (Figure 2A, LD, broken curves). CW and CCW stirring resulted in mirror-image CD spectral profiles (−560 and 370 mdeg, respectively, at 266 nm) and virtually the same LD profiles (Δo.d. (optical density) = 0.057 and 0.047 respectively, at 259 nm) with different intensities (vide infra), and the sample solution quickly responded spectroscopically to the applied changes in stirring conditions (Figure 3B). As controls, induced CD and LD responses were not observed upon stirring in a solution containing shorter DNA with low molecular weight (approximately $M_w = 0.5 \times 10^5$–1.0×10^5) (Figure S1), which may hardly sense hydrodynamic shear force of fluids beyond Brownian motions of the solvent, but analogous induced spectra with relatively weak intensities were observed in a solution of calf-thymus DNA with high molecular weight (approximately $M_w = 8.5 \times 10^6$) (Figure S2).[21] Because the increases in LD intensity gradually decreased as the DNA concentrations increased (Figure 3C), condensation of the DNA solution, which increases viscosity, may not be favored because of the decreasing hydrodynamic interaction.

CD and LD Spectroscopy of a Wet DNA Sample upon Applying Shear Forces. The results obtained with CD and LD spectroscopy indicated the macroscopic, helical alignments of DNA in the vortex, likely as a hydrodynamic behavior of flexible ribbons in the vortex (see Supporting Information, Movie 1), and are schematically illustrated in Figures 1B and 1C.[16,17] As a reference, Maestre and Reich reported that a thin film of DNA, prepared in an ethanolic buffer or upon

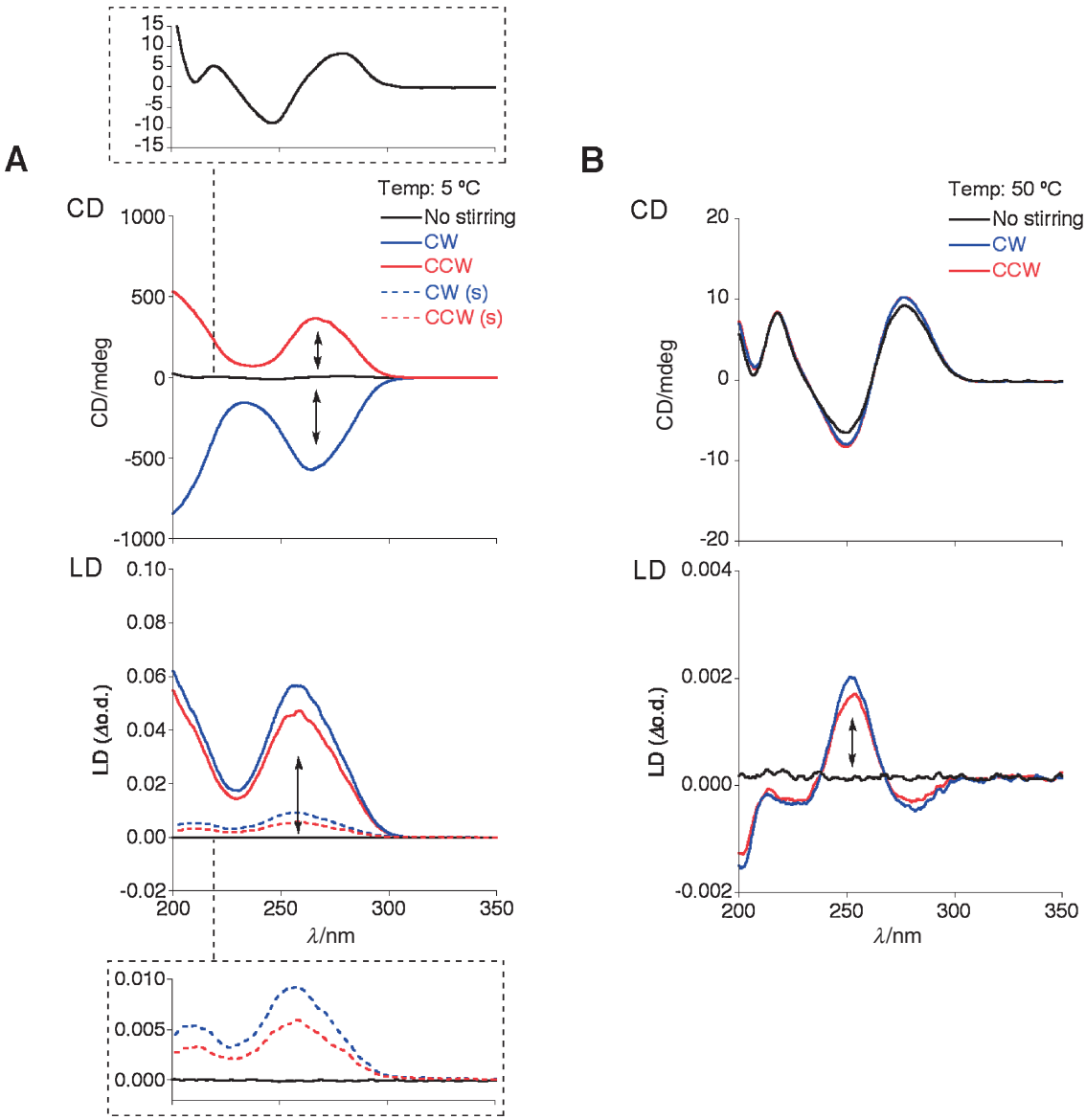

Figure 2. Circular dichroism (CD) and linear dichroism (LD) spectra of DNA dissolved in pure water induced by rotary stirring. CD (top) and LD (bottom) spectra of a solution of salmon testes DNA (5.1×10^{-2} mg mL^{-1}) dissolved in pure water at (**A**) 5 and (**B**) 50 °C upon stirring at 1350 rpm in the CW (blue curve) or CCW (red curve) direction using a $\phi 3.0 \times 8.0$ mm (solid curve) or $\phi 2.0 \times 5.0$ mm (broken curve) Teflon-coated magnetic stir bar. CD and LD spectra without stirring are indicated with black curves. Insets show the magnified CD and LD spectra obtained without stirring and upon stirring with the $\phi 2.0 \times 5.0$ mm stir bar, respectively. CD and LD spectra were recorded from solution (3.0 mL) stored in a $10 \times 10 \times 40$ mm^3 quartz optical cell.

complexation with polylysine, can provide opposite CD responses upon CW or CCW twisting of a sample sandwiched between two quartz plates.[22] In order to assess the above intriguing CD effect, we also demonstrated CD and LD spectroscopy upon twisting or slipping of a wet DNA sample (33 mg mL^{-1}) sandwiched by $40 \times 10 \times 1$ mm^3 quartz glass plates (Figure 4).[23] Quite interestingly, the sample after rotation of the glass plates in CW or CCW direction provided mirror imaged CD responses (Figure 4A), whose spectral shapes are virtually identical to those observed for the stirred solutions of DNA at low temperature (Figure 2A). As expected, the sample also showed LD activity upon parallel vertical slip of the glass plates (Figure 4B), whose spectral pattern is also virtually the same as that observed for the stirred solutions of DNA (Figure 2A) and inverted with a horizontally slipped sample. Hence, here, the DNA molecules are oriented preferentially along the directions of shear force applied. These CD and LD spectral features indicate that the observed chiroptical activity is not at the molecular level but a macroscopic CD effect originating from the twisted geometry of the oriented DNA like mesogenic molecules in a cholesteric liquid crystalline mesophase.[24,25]

Temperature Effects. The observed CD and LD responses of the stirred sample solution decreased simultaneously as the double-stranded structure denatures with increasing temperatures. The temperature-dependent CD and LD profiles are

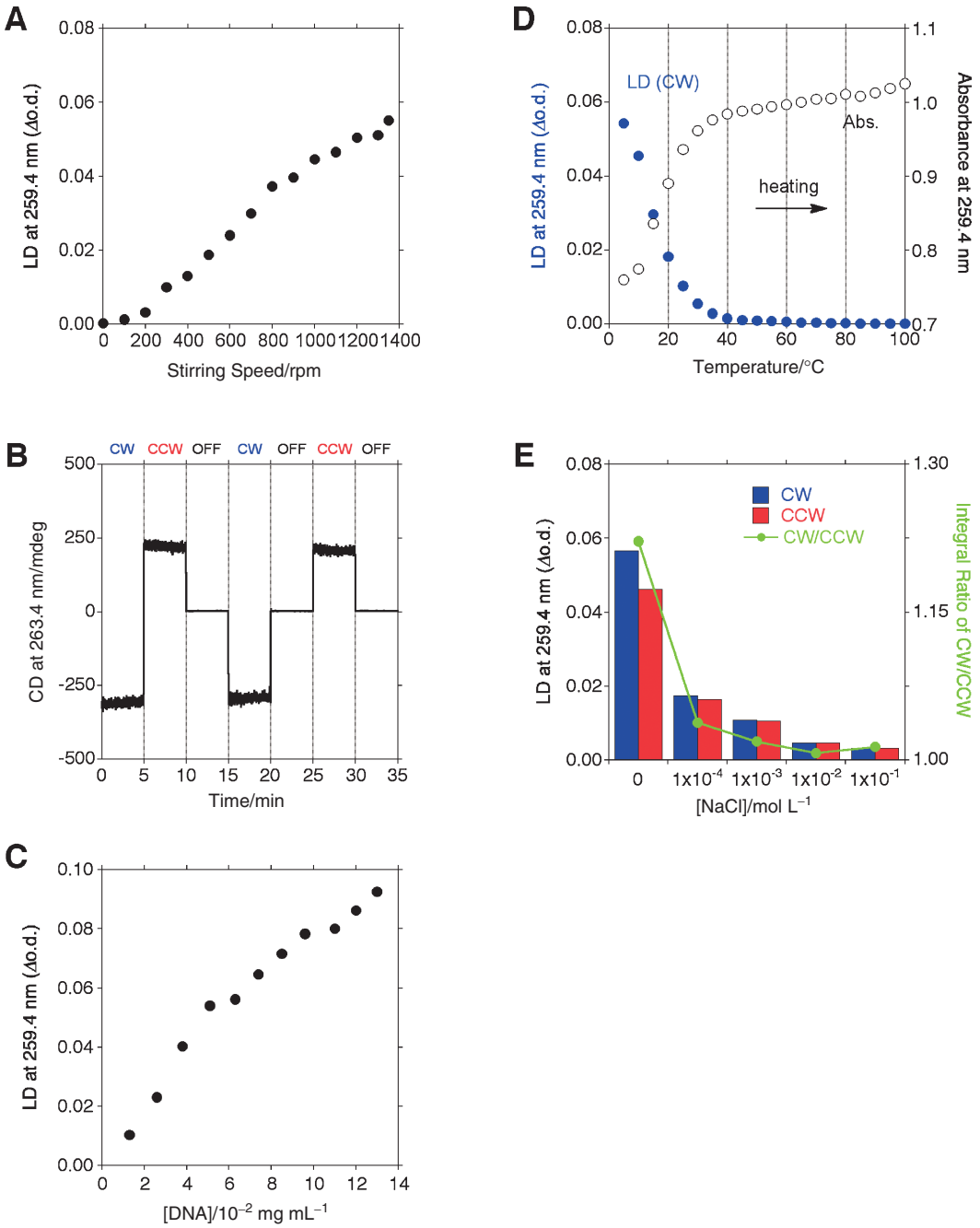

Figure 3. Changes in spectral intensities as conditions, concentration, temperature, and salt-concentration vary. (**A**) Changes in LD intensity at 259.4 nm in response to stirring speed. (**B**) Changes in CD intensity at 263.4 nm in response to sequential variation of the stirring conditions. (**C**) DNA concentration-dependence (1.3×10^{-2}–13.0×10^{-2} mg mL^{-1}) of LD intensity obtained upon CW stirring and (**D**) temperature-dependence (5–100 °C) of LD intensity (blue filled circle) and absorbance (black open circle) of a DNA solution. (**E**) Changes in LD intensities (blue and red bars represent CW and CCW stirring, respectively) and integral ratios of the LD absorption bands (250–300 nm) of CW/CCW stirring (greenish brown curve) of a DNA solution upon addition of NaCl. CD and LD spectra were recorded while the solution (3.0 mL) was stirred in the CW or CCW direction in a $10 \times 10 \times 40$ mm^3 quartz optical cell using a $\phi 3.0 \times 8.0$ mm Teflon-coated magnetic stir bar rotated at 1350 rpm. DNA solution was prepared at a concentration of 5.1×10^{-2} mg mL^{-1} in (**A**), (**B**), (**D**), and (**E**). Spectroscopic measurements in (**A**), (**B**), (**C**), and (**E**) were conducted at 5 °C.

essentially the same as the melting curvature obtained with absorption spectroscopy (Figures 3D and S3). The stirred sample solution at 50 °C after the denaturation provided virtually the same CD spectral pattern as the nonstirred sample, and the LD pattern of the denatured sample had a weak intensity and was entirely different than that of the double-stranded sample (Figure 2B). The inefficiently aligned single-strand DNA may provide such a weak LD spectrum because its

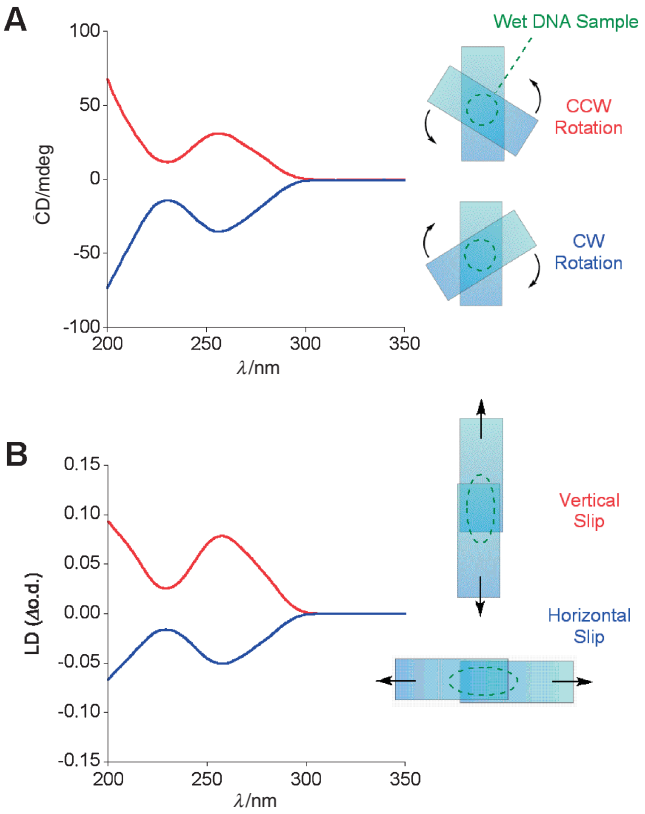

Figure 4. (**A**) CD and (**B**) LD spectra of sheared wet DNA samples sandwiched by quartz glass plates (40 × 10 × 1 mm^3). The spectroscopic measurements were demonstrated at 20 °C with a salmon testes DNA dissolved in pure water (33 mg mL^{-1}) after applying 360° rotation of the glass plates in the CW (blue curve) or CCW (red curve) direction in CD spectroscopy and vertical (red curve) or horizontal (blue curve) slip of the glass plates in LD spectroscopy.

base components are liberated from the structural restrictions caused by hydrogen bonds in the duplex. Because the double-stranded DNA showed nonsplitting LD bands at λ_{max} of 259 nm originating from parallel stacking of the base pair in the alignment, the observed bisignated LD bands at 253 and 282 nm upon dissociation indicates actually the resulting conformational changes of the base components against the aligned axis of the single-stranded DNA. These results indicate the importance of the double-stranded form, which can increase rigidity, linearity, and thickness of the DNA structure, for the hydrodynamic helical alignment in the vortex.

Ionic Effects upon Addition of NaCl or ETB. Next we addressed the effects of the ionic conditions because increasing the ionic strength of the aqueous solvent reduces the mutually repulsive forces of negative charges on the two DNA strands, therefore the elasticity, higher order structures and the denaturation temperature of the DNA molecules change (Figure 5, left).[26–29] Actually, the melting temperature of DNA increases dramatically from 20 to 85 °C in the presence of 0.1 M NaCl (Figure S4). However, intensities of the CD and LD spectra induced by stirring decreased or disappeared upon addition of NaCl and even Tris-HCl buffer, where the hydrodynamic interactions of DNA with the solvent molecules may be affected by changes in the DNA structures and/or physical properties of the solvent (Figures 3E and S5). Although Na^+ mainly interacts with phosphate anion exteriors of DNA, ETB, a cationic aromatic polycycle, is an intercalator (Figure 5, right).[30,31] The DNA dynamically accommodates multiple molecules of ETB into the spaces between its base pairs by unwinding, which induces local structural changes to the double-stranded DNA (e.g., lengthening and hardening) and a variety of functional changes. The melting temperature of DNA in water actually changed to ≈95 °C in the presence of 3.2×10^{-2} mM ETB (0.39 equiv for each DNA base pair) (Figure 6B, black open circles). In comparison with the cases of NaCl and without additives, no notable changes in intensities of either the CD or LD spectra were observed in the solution as the concentration of ETB increased (Figure 6C), but the spectra had new bands in the range of 400 to 580 nm and shoulders of a DNA bands at around 300 to 350 nm that originated from the intercalated ETB (Figure 6A).[32] As expected, ETB alone did not result in either a CD or LD response. The temperature-dependent absorption and LD spectral measurements of the mixture of DNA and ETB, monitored at 259.4 and 260.0 nm, respectively, showed synchronous changes in their profiles from 5 to 100 °C (Figure 6B). The thermal fluctuations of the DNA double strand, which accelerates the intercalation of ETB by unwinding at low temperature, may provide the nonlinear profiles observed from 5 to 80 °C, and then, the denaturation of DNA as the ETB dissociates at higher temperature results in an increase and disappearance of the absorption and LD responses, respectively (Figure S6). In the mid region of 20–80 °C, where the induced LD intensity gradually decreases without absorbance change in UV–vis spectrum with increasing temperature, the hydrodynamic interactions between DNA and solvent molecules may also respond to the changes in the DNA structures and/or physical properties of the solvent. Hence, DNA can thermally stabilize its structure without changes of flowing character upon complexation with ETB.

LD Spectroscopy of a DNA Solution upon Rotary CW or CCW Stirring. These experimental results highlight the observed differences in spectral intensities generated by CW and CCW stirring. CW stirring, which generates right-handed torsional flows, always resulted in larger spectral intensities in both CD and LD spectroscopy than CCW stirring. Because CD spectra, applied to anisotropic macromolecules, may be contaminated by LD as an intrinsic artifact,[18,33] quantitative treatments of the chiroptical features of aligned DNA will occasionally be misleading. Hence, the observed difference should be discussed using LD spectral studies. Although we initially suspected that instrumental errors in spectroscopy were influencing our observations, no notable differences in intensity upon CW and CCW stirring were observed in our previous studies of nanofibers composed of self-assembled zinc porphyrin derivatives (Figures S7 and S8).[16,19] With the assumption that observed differences originate from an intrinsic difference in the torsional elasticity of DNA in right- and left-handed hydrodynamic forces (Figure 1D),[11–15] we carried out LD spectral measurements with rigidly stabilized DNA in the presence of NaCl or ETB. When integral ratios of the LD bands obtained by CW and CCW stirring in the range of 250 to

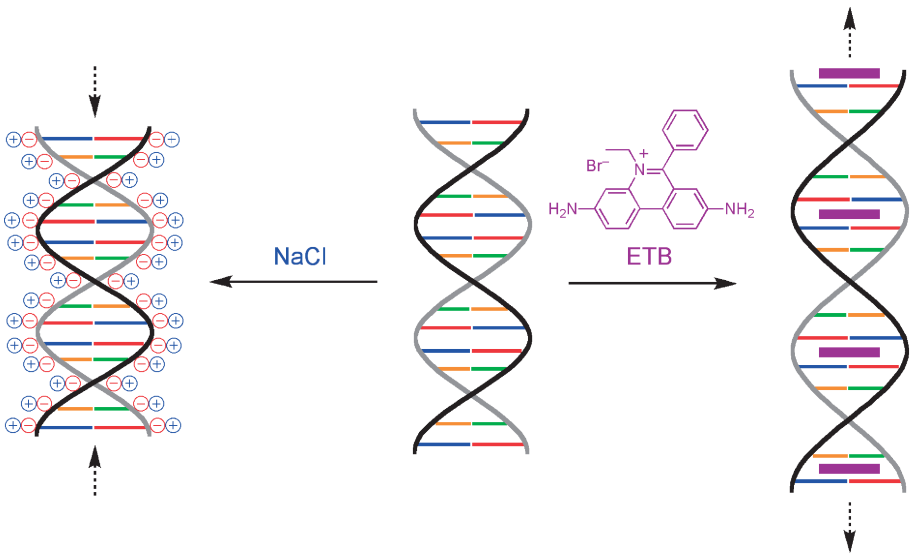

Figure 5. Schematic illustration of DNA structures upon interaction with Na^+ at phosphate anion exteriors (left) and intercalation with ETB inside of the base pairs (right).

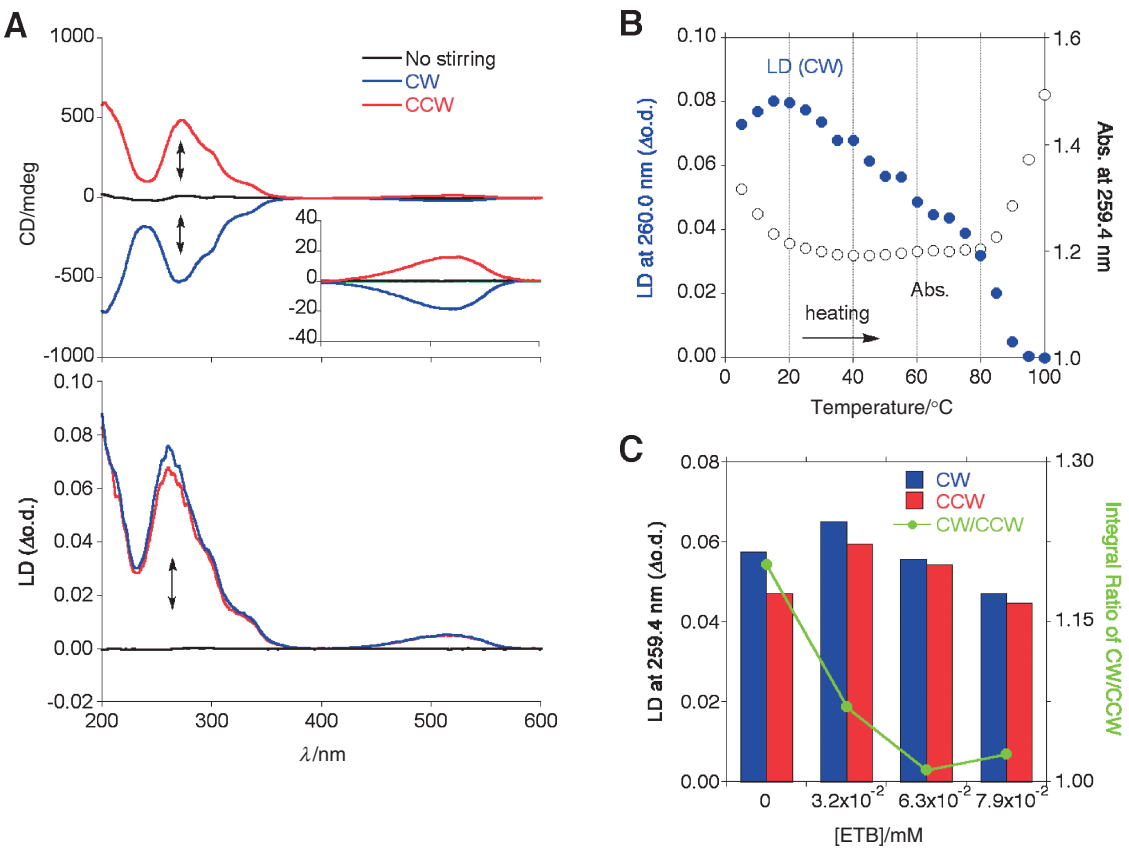

Figure 6. CD and LD spectroscopy of a solution of DNA/ETB complexes in pure water. (**A**) CD (top) and LD (bottom) spectra of a solution containing a mixture of DNA (5.1×10^{-2} mg mL^{-1}) and ETB (3.2×10^{-2} mM, 0.39 equiv for DNA base pair) in water; the solutions were stirred at 1350 rpm in either the CW (blue curve) or CCW (red curve) direction using a $\phi 3.0 \times 8.0$ mm Teflon-coated magnetic stirrer bar, or they were not stirred (black curve). (**B**) Temperature dependence (5–100 °C) of LD intensity (blue filled circle) and absorbance (black open circle) of the sample solution. (**C**) Changes in LD intensities (blue and red bars represent CW and CCW stirring, respectively) and integral ratios of the LD spectra (250–300 nm) of CW/CCW stirring (greenish brown curve) of the DNA solution upon addition of ETB. CD and LD spectra were recorded while the solution (3.0 mL) was stirred in a $10 \times 10 \times 40$ mm^3 quartz optical cell. Spectroscopic measurements in (**A**) and (**C**) were conducted at 20 °C.

300 nm was plotted with respect to the concentration of NaCl (≈0.1 M), a CW/CCW ratio of 1.22 initially attained at 5 °C in pure water as solvent was found to decrease with higher NaCl concentrations; the ratio fell to 1.01 at 0.1 M NaCl (Figure 3E, greenish brown curve). Further, the CW/CCW ratio was also decreased upon addition of ETB and fell to 1.03 at 7.9×10^{-2} mM ETB (Figure 6C, greenish brown curve). These results may be explained by the expectation that the relaxed coil should have larger differences in its chiral twist elasticity for CW and CCW directions than that of a rigid coil. The differences may allow the observed hydrodynamic preference of DNA for right- or left-handed torsional flows. However, a larger CW/CCW value (1.59) was attained with a smaller ($\phi 2.0 \times 5.0$ mm) stir bar, which can generate a narrow torsional flow at the center of the vortex (Figure 2A, broken curves). Decreases in the scale gap between the DNA and the torsional flow may enhance the present chiral hydrodynamic interaction.

Conclusion

In the present study, the combined CD and LD spectroscopy allowed spectroscopic visualization of the dynamic helical alignment of DNA molecules in macroscopic chiral vortex flows. DNA in water without additives was found to align helically in the vortex and well order in the right-handed vortex rather than the left-handed one. These novel observations suggested that the chiral hydrodynamic interactions between the asymmetric biomolecules and fluids are important in natural biological systems.

Experimental

Materials. Sodium salts of DNA from salmon testes and calf-thymus were purchased from Sigma and used without farther purification. Ethidium bromide (95%) was purchased from Nacalai Tesque.

Measurements. DNA solutions were prepared with Millipore purified ultrapure water, and stored at 3 °C. CD and LD spectra were recorded on a JASCO J-820 spectropolarimeter equipped with a JASCO PTC-423L temperature/stirring controller and a custom made CW/CCW-stirring system. The spectrometer is equipped with a $10 \times 10 \times 40\,\text{mm}^3$ quartz optical cell, in which sample solutions (3 mL) are stirred mechanically using a $\phi 3.0 \times 8.0$ mm or $\phi 2.0 \times 5.0$ mm Teflon-coated magnetic stirrer bar at the bottom of the cell, 14 mm below the center of a $\phi 8.0$ mm wide polarized light pass. LD intensity is defined as $\Delta_{LD}A = A_{//} - A_{\perp}$ ($\Delta_{LD}A$ represents magnitude of LD, while $A_{//}$ and $A_{\perp}$ denote horizontal and perpendicular absorbances, respectively). Electronic absorption spectra were recorded using a JASCO V-670 UV/VIS/NIR spectrometer equipped with a JASCO ETC-717 temperature/stirring controller.

The present work was sponsored by a Grant-in-Aid for Scientific Research (B) (No. 22350061) from the Ministry of Education, Culture, Sports, Science and Technology, Japan, by Japan Science and Technology Agency, Research Seeds Program, by the Asahi Grass Foundation and by TEPCO Research Foundation, and the Toray Science and Technology Grant. The authors thank Prof. K. Koumoto for his helpful comments through prior examination of the manuscript.

Supporting Information

CD, LD, and absorption spectroscopy, supporting movie, and control experiments. This material is available free of charge on the web at http://www.csj.jp/journals/bcsj/.

References

1 S. B. Smith, L. Finzi, C. Bustamante, *Science* **1992**, *258*, 1122.

2 T. T. Perkins, D. E. Smith, R. G. Larson, S. Chu, *Science* **1995**, *268*, 83.

3 J. Jing, J. Reed, J. Huang, X. Hu, V. Clarke, J. Edington, D. Housman, T. S. Anantharaman, E. J. Huff, B. Mishra, B. Porter, A. Shenker, E. Wolfson, C. Hiort, R. Kantor, C. Aston, D. C. Schwartz, *Proc. Natl. Acad. Sci. U.S.A.* **1998**, *95*, 8046.

4 a) B. Nordén, C. Elvingson, M. Jonsson, B. Åkerman, *Q. Rev. Biophys.* **1991**, *24*, 103. b) R. Marrington, T. R. Dafforn, D. J. Halsall, J. I. MacDonald, M. Hicks, A. Rodger, *Analyst* **2005**, *130*, 1608. c) B. Nordén, A. Rodger, T. Dafforn, *Linear Dichroism and Circular Dichroism: A Textbook on Polarized-Light Spectroscopy*, 1st ed., Royal Society of Chemistry, Cambridge, **2010**.

5 J. Rajendra, M. Baxendale, L. G. D. Rap, A. Rodger, *J. Am. Chem. Soc.* **2004**, *126*, 11182.

6 J. F. Marko, E. D. Siggia, *Science* **1994**, *265*, 506.

7 F. R. Hama, J. Nutant, *Phys. Fluids* **1961**, *4*, 28.

8 S. F. Mason, *Nature* **1984**, *311*, 19.

9 D. K. Kondepudi, R. J. Kaufman, N. Singh, *Science* **1990**, *250*, 975.

10 a) O. Ohno, Y. Kaizu, H. Kobayashi, *J. Chem. Phys.* **1993**, *99*, 4128. b) J. M. Ribó, J. Crusats, F. Sagués, J. Claret, R. Rubires, *Science* **2001**, *292*, 2063. c) C. Escudero, J. Crusats, I. Díez-Pérez, Z. El-Hachemi, J. M. Ribó, *Angew. Chem., Int. Ed.* **2006**, *45*, 8032. d) Z. El-Hachemi, O. Arteaga, A. Canillas, J. Crusats, C. Escudero, R. Kuroda, T. Harada, M. Rosa, J. M. Ribó, *Chem.—Eur. J.* **2008**, *14*, 6438.

11 T. R. Strick, J.-F. Allemand, D. Bensimon, A. Bensimon, V. Croquette, *Science* **1996**, *271*, 1835.

12 P. R. Selvin, D. N. Cook, N. G. Pon, W. R. Bauer, M. P. Klein, J. E. Hearst, *Science* **1992**, *255*, 82.

13 Z. Bryant, M. D. Stone, J. Gore, S. B. Smith, N. R. Cozzarelli, C. Bustamante, *Nature* **2003**, *424*, 338.

14 S. Neukirch, *Phys. Rev. Lett.* **2004**, *93*, 198107.

15 M. D. Stone, Z. Bryant, N. J. Crisona, S. B. Smith, A. Vologodskii, C. Bustamante, N. R. Cozzarelli, *Proc. Natl. Acad. Sci. U.S.A.* **2003**, *100*, 8654.

16 a) A. Tsuda, M. A. Alam, T. Harada, T. Yamaguchi, N. Ishii, T. Aida, *Angew. Chem., Int. Ed.* **2007**, *46*, 8198. b) D. B. Amabilino, *Nat. Mater.* **2007**, *6*, 924. c) G. P. Spada, *Angew. Chem., Int. Ed.* **2008**, *47*, 636.

17 M. Wolffs, S. J. George, Ž. Tomović, S. C. J. Meskers, A. P. H. J. Schenning, E. W. Meijer, *Angew. Chem., Int. Ed.* **2007**, *46*, 8203.

18 Å. Davidsson, B. Nordén, S. Seth, *Chem. Phys. Lett.* **1980**, *70*, 313.

19 A. Tsuda, Y. Nagamine, R. Watanabe, Y. Nagatani, N. Ishii, T. Aida, *Nat. Chem.* **2010**, *2*, 977.

20 K. Tanaka, Y. Okahata, *J. Am. Chem. Soc.* **1996**, *118*, 10679.

21 B. Porsch, R. Laga, J. Horský, C. Konák, K. Ulbrich, *Biomacromolecules* **2009**, *10*, 3148.

22 M. F. Maestre, C. Reich, *Biochemistry* **1980**, *19*, 5214.

23 a) R. Brandes, D. R. Kearns, *Biochemistry* **1986**, *25*, 5890. b) G. P. Spada, P. Brigidi, G. Gottarelli, *J. Chem. Soc., Chem. Commun.* **1988**, 953.
24 J. Schellman, H. P. Jensen, *Chem. Rev.* **1987**, *87*, 1359.
25 F. D. Saeva, J. J. Wysocki, *J. Am. Chem. Soc.* **1971**, *93*, 5928.
26 C. G. Baumann, S. B. Smith, V. A. Bloomfield, C. Bustamante, *Proc. Natl. Acad. Sci. U.S.A.* **1997**, *94*, 6185.
27 M. Saminathan, T. Antony, A. Shirahata, L. H. Sigal, T. Thomas, T. J. Thomas, *Biochemistry* **1999**, *38*, 3821.
28 K. Miwa, Y. Furusho, E. Yashima, *Nat. Chem.* **2010**, *2*, 444.
29 N. G. Hunt, J. E. Hearst, *J. Chem. Phys.* **1991**, *95*, 9329.
30 D. Freifelder, *J. Mol. Biol.* **1971**, *60*, 401.
31 S. F. Yen, E. J. Gabbay, W. D. Wilson, *Biochemistry* **1982**, *21*, 2070.
32 M. Balaz, M. De Napoli, A. E. Holmes, A. Mammana, K. Nakanishi, N. Berova, R. Purrello, *Angew. Chem., Int. Ed.* **2005**, *44*, 4006.
33 Y. Shindo, M. Nishio, S. Maeda, *Biopolymers* **1990**, *30*, 405.